

# Nanoscale

Accepted Manuscript



This is an *Accepted Manuscript*, which has been through the Royal Society of Chemistry peer review process and has been accepted for publication.

*Accepted Manuscripts* are published online shortly after acceptance, before technical editing, formatting and proof reading. Using this free service, authors can make their results available to the community, in citable form, before we publish the edited article. We will replace this *Accepted Manuscript* with the edited and formatted *Advance Article* as soon as it is available.

You can find more information about *Accepted Manuscripts* in the [Information for Authors](#).

Please note that technical editing may introduce minor changes to the text and/or graphics, which may alter content. The journal's standard [Terms & Conditions](#) and the [Ethical guidelines](#) still apply. In no event shall the Royal Society of Chemistry be held responsible for any errors or omissions in this *Accepted Manuscript* or any consequences arising from the use of any information it contains.



Journal Name

ARTICLE

## Transparent and Through thickness Conductive Polystyrene films Using External magnetic fields for “Z” alignment of Nickel nanoparticles

Received 00th January 20xx,  
Accepted 00th January 20xx

DOI: 10.1039/x0xx00000x

www.rsc.org/

Yuwei Chen<sup>a,b</sup>, Yuanhao Guo<sup>a</sup>, Saurabh Batra<sup>a</sup>, Enmin Wang<sup>a</sup>, Yanping Wang<sup>b</sup>, Xueqing Liu<sup>c</sup>, Yimin Wang<sup>b</sup>, Miko Cakmak<sup>\*a</sup>

Combination of transparency, electrical conductivity and flexibility are desired in emerging flexible electronics industry for current and future applications. In this paper, we report the development of through thickness electrical conductivity in polystyrene films filled with nickel nanopowders by external magnetic field application. This process leads to the formation of nanocolumns of nickel spanning across the thickness direction while generating nanoparticle depleted regions in between. This leads to directionally dependent enhancement in optical light transmission particularly in normal direction of the films. With the use of as little as 2 wt. % (0.22 vol %) nickel we were able to achieve high through thickness conductivity under the influence of magnetic field. While these films exhibit high through thickness conductivity they remain non-conductive in their planes as a result of the unique nanomorphology created which eliminates potential side branch formations. These films are anticipated to be used as electrodes for touch screens, electric dissipative materials for electronic packaging and other sensors.

### Introduction

Electrically conductive polymer composites have received much attention owing to their unique electrical, mechanical and optical properties.<sup>1,2</sup> They usually comprise of electrically conductive particles such as various forms of carbons<sup>3-6</sup> and metals<sup>7-9</sup> dispersed in an insulating polymer matrix and have been adapted to variety of applications including electromagnetic interference (EMI), electrostatic dissipation (ESD), electronic packaging (ICAs: Isotropic Conductive Adhesives; ACAs: Anisotropic Conductive Adhesives) etc.<sup>10,11</sup> Both carbon based materials and metals have high intrinsic conductivity, however, normally conductive fillers are randomly distributed in polymer matrix, at low filler content the conductive particles are well separated and the composite is insulating.<sup>12</sup> The conductivity arises when the

conductive particle concentration reaches a critical value called percolation threshold that leads to formation of continuous pathways of conductive filler throughout the insulating polymer matrix.<sup>10</sup> For random distribution of conductive powders in a non-conductive medium, the percolation threshold is usually higher than 10 vol.%,<sup>12,13</sup> as these conductive particles form unconnected branches that do not contribute to the overall conductivity, leading to increased light absorption making the materials opaque. Much effort has been devoted to minimizing the conductive filler concentration for variety of reasons including cost and transparency and mechanical flexibility. Low percolation threshold occurs in anisotropic composites when chains of conductive filler are assembled during processing, by the application of electric field<sup>14-16</sup>, magnetic field<sup>17-20</sup>, shear force<sup>1,21-23</sup> etc. Magnetic fields are particularly attractive for realization of an externally imposed magnetic driving force in any shape mold without any geometric constraints encountered with other fields like electric field or mechanical shear. Moreover, the use of magnetic field, enables formation of vertically aligned structures in thin film geometries in the absence of electrode

<sup>a</sup> Polymer Engineering Department, The University of Akron, Akron OH 44325-0301  
Email: Cakmak@uakron.edu

<sup>b</sup> State Key Laboratory for Modification of Chemical Fibers and Polymer Materials, College of Materials Science and Engineering, Donghua University, Shanghai 201620

<sup>c</sup> Key Laboratory of Optoelectronic Chemical Material and Devices of Ministry of Education, Jiangnan University, Wuhan 430056, PR China

contact without dielectric breakdown concerns that are particular concerns in electric field alignment.<sup>24,25</sup>

The mechanism of magnetic field-induced assembly of molecular chain,<sup>26-28</sup> a phase of block copolymer,<sup>25,29</sup> diamagnetic particles,<sup>17,30,31</sup> ferromagnetic particles (nickel, cobalt, iron)<sup>2,32,33</sup> have been well studied. For the magnetic field induced-alignment of chain and phase and diamagnetic particles, the mechanism is that polymer chain or phase or diamagnetic particles can interact with a magnetic field caused by the diamagnetic anisotropy of its constituent repeating units. The units tend to align in a certain direction that optimizes the energy reduction since the energy that the repeating unit gains through the interaction with an external magnetic field is dependent on the orientation of the unit relative to the magnetic field.<sup>28,34</sup> A positive diamagnetic anisotropy leads to alignment of the molecular chain or phase along an axis parallel to applied magnetic field. Negative diamagnetic anisotropy leads to alignment along the direction perpendicular to magnetic field.<sup>28,30,35</sup> Magnetic field-induced alignment of these system only can proceed at relatively high magnetic field to provide required driving force to reorientation since the anisotropy of susceptibility is usually a vanishingly small. Relatively low magnetic fields are required to align ferromagnetic particles as their magnetic susceptibility are far higher than diamagnetic materials. Therefore magnetic field-induced alignment of ferromagnetic particles is an effective and low cost means to achieve nanocolumnar structure oriented in thickness ("Z" direction) and resulting anisotropic properties.

Although many publications on other technologies processing anisotropic conductive films have been reported,<sup>23,36-42</sup> new technology of processing anisotropic conductive materials that satisfies the additional requirements such as transparency, electrical conductivity, low material cost, low processing cost for thin film formation, and capability of manufacturing a large-area sheet has not been reported.

Recently, we developed a novel roll-to-roll (R2R) processing line that can cast polymer solutions and monomers filled with functional particles and orient and align these functional particles in polymer phases using external electric, magnetic,

and thermal gradient fields.<sup>43-45</sup> This roll-to-roll processing line could be used to reduce the cost of manufacturing by limiting the amount of functional fillers through directional alignment leading to "directed percolation" while enhancing the properties in thickness direction at low filler concentrations. In this study, we present our results on the influence of magnetic field on the formation of nanostructural hierarchy and resulting anisotropic electrical conductivities.

## Results and discussion

In order to assess the development of particle orientation in thickness direction ("Z-oriented morphology"), we have focused our studies on low concentrations of nickel filler in PS solutions.

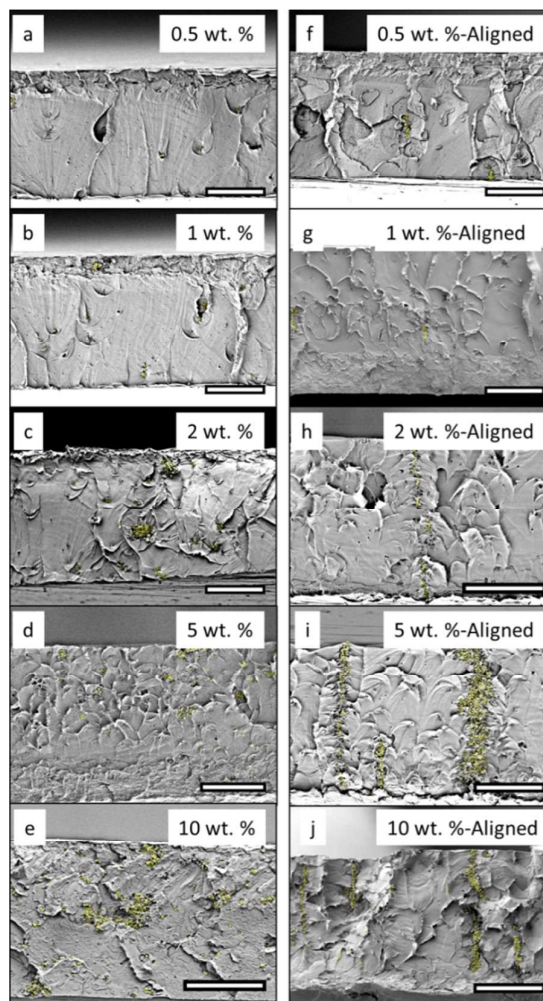


**Fig. 1** Preferred orientation in Ni powder/PS as a function of Ni loading. (Scale bar: 50  $\mu\text{m}$ )

Fig. 1 shows scanning electron micrographs of non-aligned and aligned films for selected particle fractions. Transparent yellow circles are placed on the Ni particles and aggregates to enhance the micrographs. For Ni/PS composite processed without magnetic field (Fig.1 a-e), no chain structure was observed. For low particle concentration samples (0.5 wt. %), they form particle chains whose axes oriented in the thickness direction but they do not span the full thickness. (Fig.1 f, g). Above about 2 wt. %, the particles form aligned chains long enough to span the full film thickness (Fig.1 h). More pathways throughout the thickness direction formed as the particle fraction increased (Fig.1 i, j). We also observe that these particle chains (columns) break through the upper surface leading to formation of protrusions like nano-needles as shown in Fig. 2. In order to understand the three dimensional distribution of these chains(columns), micro computed tomography was utilized to obtain 3D image of 10 wt.% Ni powder/PS, Fig. 3 shows that the Ni powder stand up like rods whose axes oriented in thickness direction of PS matrix.

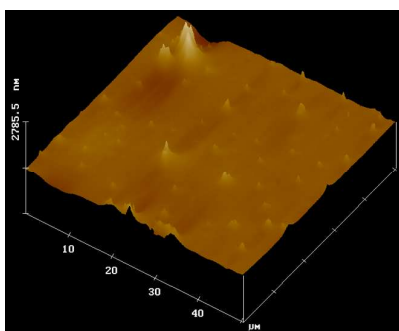


**Fig. 2** Surface morphology of 10wt% Ni powder/PS

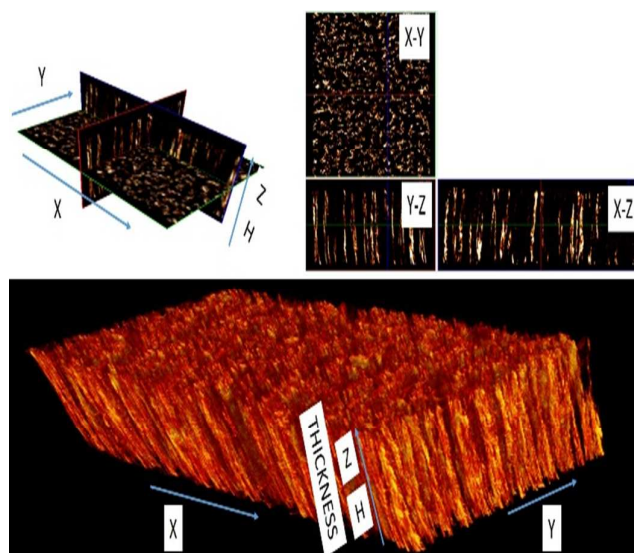


**Fig. 3** Micro Computed Tomography of the preferential orientation of 10 wt. % Ni powder/PS.

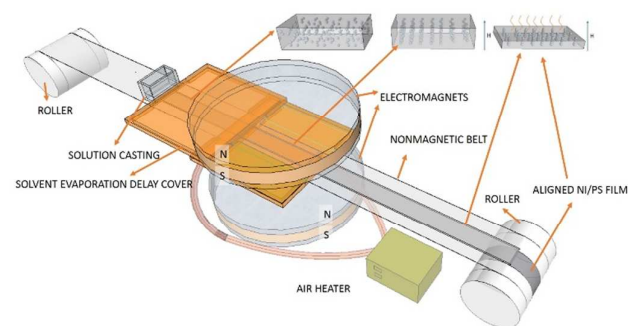


**Fig. 4** A schematic model for showing the roll to roll magnetic alignment process.

Fig. 4 shows the schematic of the particle organizations under the influence of magnetic field and as a result of shrinkage due to evaporation of solvent. The randomly dispersed particles in the polymer solution were aligned by passing them through gap between the poles of electromagnet that organize these particles along nanocolumns. The shrinkage induced by solvent evaporation leads to the decrease of particle-to-particle distance and enhancement of electrical conductivity. The alignment was observed by optical microscopy, the video captured during the alignment shows that this organization takes place in seconds (Video available in supporting information) where the in-plane alignment of these nanoparticles with permanent magnets in optical microscopy

is shown. With the available heating system the solvent can be evaporated at a reasonable rate. Since the solvent evaporation takes tens of minutes that can be adjusted by heating assembly near the electromagnets, there is enough time for Ni complete the alignment before the polymer matrix is solidified.

In the presence of the magnetic field, each particle placed in solution is magnetized along the field direction. Since all dipoles are aligned in magnetic field direction, they repel each other in the transverse direction and attract each other along the field direction. Based on magnetic hysteresis, the magnetization of Ni particle is increased with the increase of external magnetic field until the saturation field is reached. Since the saturation field of Ni particle is roughly  $3T$ <sup>32</sup>, magnetic dipole moments and the strength of the magnetic interaction between particles are increasing with the increase of magnetic field in the range of 0-3T. As indicated in Fig. 5, the length of Ni chains increases with applied magnetic field strength goes up. When the external magnetic field intensity is high enough, the chains form and when they grow long enough they span between the two surfaces leading electrical and thermal conductivity in thickness direction.

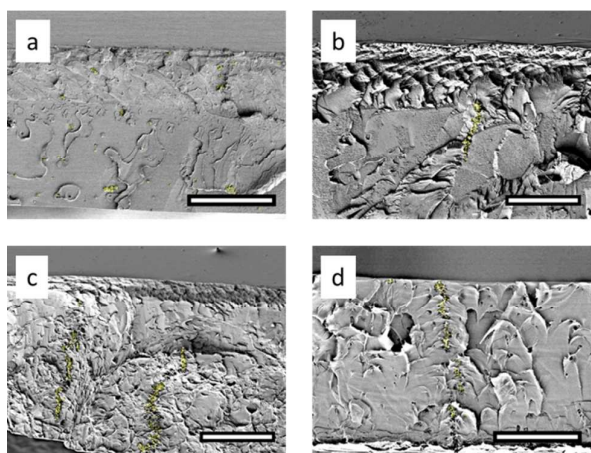


**Fig. 5** Cross section of 2 wt. % Ni powder/PS aligned by varying magnetic intensity. a) 0T; b) 0.02T; c) 0.1T; d) 0.2T. (Scale bar: 50  $\mu$ m)

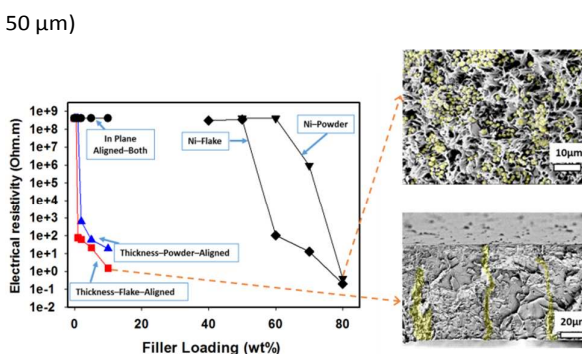


**Fig. 6** Resistivity of Ni/PS composite film.

Particle organization and alignment along nanocolumns lead to a significant conductivity enhancement along the thickness direction as shown in Fig. 6. The resistivity along Ni chain direction (out of plane) is as low as  $10^1$  ohm·m at 10 wt.% Ni powder loading, while the in plane resistivity is as high as  $1e8$  ohm·m. The resistivity anisotropy ratio is calculated to be greater than  $10^8:1$ . The percolation threshold of Ni powder/PS is about 2 wt. % compared to 80 wt. % of randomly dispersed Ni powder/PS where a conductive net of Ni powders formed inside polymer at that high particle loading, as shown in Fig. 6. In Ni/epoxy resin composites and copper/epoxy resin composites, the critical percolation concentration are 8.5 v. % and 5 v. %, respectively<sup>7</sup>. In this work, high electrical conductivity can be achieved in the thickness direction with the use of as little as 2 wt. % (0.2 v. %). To reach the same conductivity, we needed to add 80 wt. % for randomly distributed particles. The electrical resistance for pure Ni is  $6.99 \times 10^{-8}$  ohm·m, and 10 ohm·m can be achieved for 10 wt. % Ni/PS composites with aligned Ni particle chains.

The percolation threshold of Ni flake/PS is much lower than Ni powder/PS. It is due to flakes having larger surface area which enable them to form enhanced long range network connectivity than powders. Ni flakes have broader surfaces and this lead to higher contact and/or tunnelling conduction efficiency(Fig. 7a) as compared to irregular shaped Nickel nanoparticles(Fig. 7b). Thus Ni flakes can achieve percolation threshold at much lower particle concentration. A schematic illustration of the connection difference between particles is presented in Fig. 7.

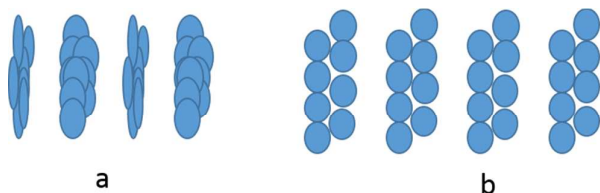


**Fig. 7** Schematic illustration of the connection between particles: a) connection between flakes; b) connection between powders.

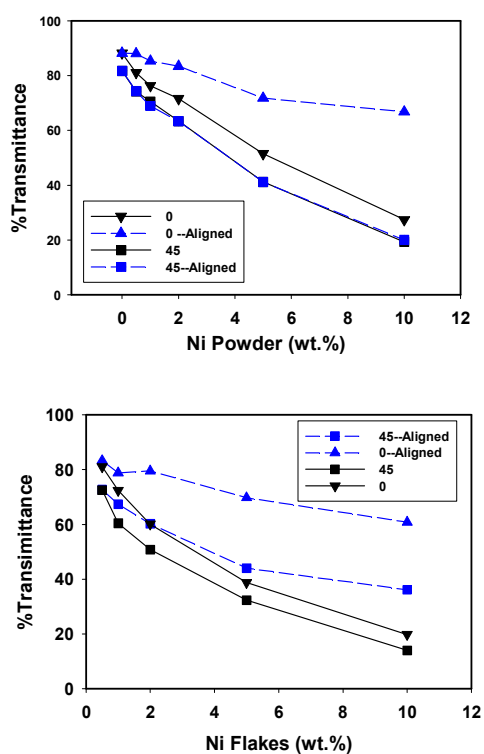


**Fig. 8** Anisotropic optical transmittance of Ni/PS film. (Wavelength: 547nm)

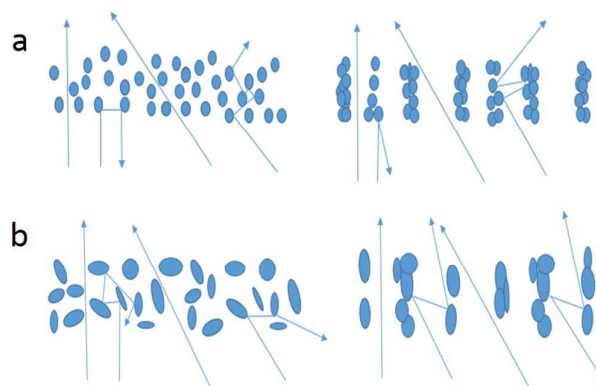


**Fig. 9** Schematic illustration of the light passing through Ni/PS composite film: a) Ni powder/PS; b) Ni flake/PS.

Formation thickness oriented Ni chain nanocolumnar structure not only provides Ni/PS composites with anisotropic electric resistivity, but also anisotropic optical transmittance. The transmittance of Ni/PS composites prepared from both powders and flakes are measured over a wide range of filler loadings. Experimental data are shown in Fig. 8 as a function of loading. For both Ni powder/PS and Ni flake/PS, the normal transmittance ( $0^\circ$  transmittance) of aligned Ni/PS composite film was increased more than 60 % as compared to nonaligned composite containing the same 10 wt. % Ni loading. As illustrated in Fig. 9, when Ni powder or Ni flake aligned in PS, the  $0^\circ$  incident light has greater probability to pass through Ni/PS composite without encountering non-transparent Ni particles. However, when incident angle is  $45^\circ$  (seen in Figure 8), the transmittance was not increased as much as  $0^\circ$  after alignment. The alignment of Ni powders in Z direction to form columns creates transparent channels (pure PS matrix) between them. These channels are oriented in normal direction, so the light can pass through the thickness of film directly. Therefore, great enhancement of light transmission can be achieved in normal incidence ( $0^\circ$ ) after alignment of Ni powders along nanocolumns creating particle depleted zone between them. While for  $45^\circ$  light transmission, there is an angle between the transparent channels and light path. The light can't pass through the transparent channels directly, and it is blocked, absorbed and scattered by the Ni columns. Thus there's minor effect of alignment of Ni powders on the light transmission in  $45^\circ$ . This obviously leads to directional transparency. As shown in Fig. 8, the  $45^\circ$  transmittance of non-aligned Ni flake/PS only increased about 20% at 10 wt. % loading after alignment and Ni powder/PS remains essentially unchanged.

In order to understand whether the magnetic field alignment results could be accomplished under realistic manufacturing conditions, both Ni powder and Ni flake were aligned in PS using a unique custom-built roll-to-roll machine equipped with electromagnet unit (shown in Fig. 10). Fig. 11 shows the magnetic field aligned Ni/PS composite have uniform alignment structure along the film thickness direction. The roll of films produced are also shown in Fig. 11, which clearly

presents that at 10 wt.% concentration the films are essentially transparent and nanocolumnar structures obtained are uniform across and along the film casting direction as also evidenced by the uniformity of transparency throughout the unrolled portions of the films. As mentioned earlier, Ni powder filled films exhibit higher transparency as compared to nickel flakes.

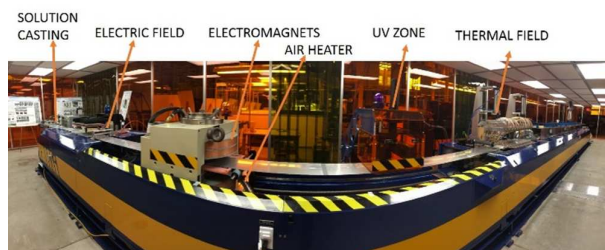


**Fig. 10** Custom-built roll-to-roll machine equipped with electric field, magnetic fields, thermal fields etc.

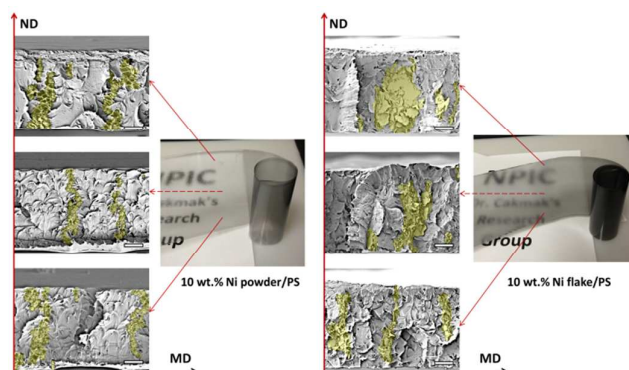


**Fig. 11** Anisotropic structure of Ni/PS processed by roll to roll manufacturing line. (Scale bar: 20  $\mu\text{m}$ )

## Conclusions

We successfully demonstrated continuous fabrication films with anisotropic electric conductivities and optical transmittance by magnetic field effect in combination with evaporation induced shrinkage facilitating Ni particles to assemble into well-ordered discrete parallel Ni nanoparticle columns assembled along the film thickness direction. This novel processing method is an efficient way to reduce the percolation threshold of the composite. We call this “directed percolation” where there essentially is no branches in the particle phase. The electrical measurement shows that the electrical resistivity along the Ni chains is 8 orders of magnitude lower than that in the film plane. In addition, anisotropic Ni chain structure also allows Ni/PS composites with anisotropic optical transmittance. For aligned Ni/PS films, the transmittance along normal ( $0^\circ$ ) incident angle is much

higher than the transmittance along  $45^\circ$  incident angle. These multifunctional films with low electrical conduction percolation threshold and anisotropic visible light transmission make them attractive for use in electronic packaging and transparent sensors.

## Experimental

**Materials.** Nickel particles were obtained from Sigma-Aldrich and Novamet Specialty Products Corp. Ni powders have a characteristic smooth surface and an average particle size of  $1\mu\text{m}$ . Ni Flakes have average 400 mesh diameter and  $1\mu\text{m}$  thickness. Polystyrene Styron 685D was used as composite matrix supplied by Styron LLC. Toluene was obtained from Sigma-Aldrich.

**Preparation of Ni/PS composite.** PS/toluene solution (30 wt. %) was prepared and added with Ni particles at 0, 1, 1.5, 2, 5 and 10 wt. % by Thinky mixer. The solution was cast by doctor blade with gap set at  $635\mu\text{m}$  on a PET substrate carried by the stainless steel belt on the roll to roll processing,<sup>43</sup> and the magnetic field was applied when the solution cast film enters in between the two poles of the 2.2 Tesla electromagnet assembled on the R2R line. Custom heating cell, shown in Fig. 12, facilitates evaporation of the solvent thus freezing the developed nanostructure. The cast film was kept under magnetic field for 10 minutes at  $100^\circ\text{C}$  until the solvent has evaporated. The final thickness of the sample is about  $120\mu\text{m}$ . The electromagnet is a GMW (Model 3474-1 40 250 mm) magnet, and the maximum magnetic field that can be achieved is 2.2 T. The magnetic field can be controlled by changing current to the magnet and field strength distribution on the belt is mapped by three-axis hall magneto meter (Model: THM1176-HF-PC) and found to be quite uniform.

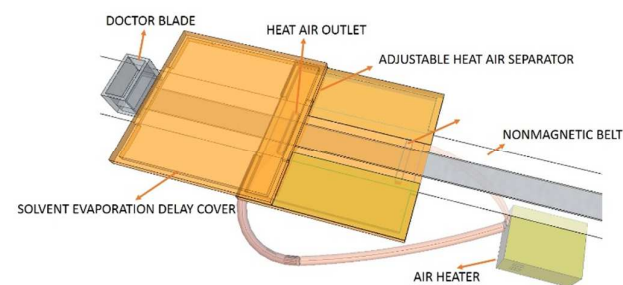


**Fig. 12.** Heating system assembled in electromagnets.

**Structural studies.** The morphology of Ni phase and protuberance formed on the film surface were observed on a field emission scanning electron microscopy (FE-SEM, HITACHI S-4800), Skyscan 1172 Micro Computed Tomography Scanner (Micro CT) and Atomic force microscope (MultiMode SPM). The typical thickness of the film was 120  $\mu\text{m}$ , the thickness of film was measured by Mitutoyo micrometer (Model: ID-S1012EBS).

**Conductivity Measurements.** In-plane direction conductivity was tested by 4-probe test device directly, while for the conductivity through the film thickness direction, film samples were placed between aluminum plates, and two probe resistance measurements were carried out using True RMS Digital Multimeter (Model: FLUKE 179). A uniaxial pressure was applied perpendicular to the planes of test samples (along the thickness direction) to obtain a good conductive contact. The resistivity  $\rho$  ( $\Omega\text{-m}$ ) was calculated from the measured resistances with the equation 1 by assuming that the volume of the sample remains constant.

$$\rho = R \frac{A}{t} \quad (1)$$

Where  $t$  is the thickness of the sample, measured in meters [m],  $A$  is the aluminum plate sample contact area [ $\text{m}^2$ ].

The visible light transmittance was measured by an instrumented apparatus described elsewhere.<sup>46</sup>

## Acknowledgements

The acknowledgements come at the end of an article after the conclusions and before the notes and references.

This work was financially supported by Third frontier Program of State of Ohio that provided funding to develop the roll to roll manufacturing line. In addition the authors gratefully acknowledge the doctoral innovation fund and scholarship of Donghua University and China scholarship council.

## Notes and references

- J. R. Lu, W. G. Weng, X. F. Chen, D. J. Wu, C. L. Wu and G. H. Chen, *Advanced Functional Materials*, 2005, **15**, 1358-1363.
- M. Knaapila, H. Høyer, J. Kjelstrup-Hansen and G. Helgesen, *ACS applied materials & interfaces*, 2014, **6**, 3469-3476.
- I. Balberg, *Carbon*, 2002, **40**, 139-143.
- F. Gubbels, R. Jérôme, P. Teyssie, E. Vanlathem, R. Deltour, A. Calderone, V. Parente and J.-L. Brédas, *Macromolecules*, 1994, **27**, 1972-1974.
- M. Ghislandi, E. Tkalya, B. Marinho, C. E. Koning and G. de With, *Composites Part A: Applied Science and Manufacturing*, 2013, **53**, 145-151.
- H. Hu, G. Zhang, L. Xiao, H. Wang, Q. Zhang and Z. Zhao, *Carbon*, 2012, **50**, 4596-4599.
- Y. P. Mamunya, V. V. Davydenko, P. Pissis and E. V. Lebedev, *European Polymer Journal*, 2002, **38**, 1887-1897.
- Q. Xue, *European Polymer Journal*, 2004, **40**, 323-327.
- I. Krupa, V. Cecen, A. Boudenne, J. Prokeš and I. Novák, *Materials & Design*, 2013, **51**, 620-628.
- J. Glatz-Reichenbach, *Journal of Electroceramics*, 1999, **3**, 329-346.
- M. J. Yim, Y. Li, K.-s. Moon, K. W. Paik and C. Wong, *Journal of adhesion science and technology*, 2008, **22**, 1593-1630.
- D. Bloor, K. Donnelly, P. Hands, P. Laughlin and D. Lussey, *Journal of Physics D: Applied Physics*, 2005, **38**, 2851.
- R. Strumpler, *Journal of Electroceramics*, 1999, **3**, 329-346.
- C. A. Martin, J. K. W. Sandler, A. H. Windle, M. K. Schwarz, W. Bauhofer, K. Schulte and M. S. P. Shaffer, *Polymer*, 2005, **46**, 877-886.
- J. Ramón-Azcón, S. Ahadian, M. Estili, X. Liang, S. Ostrovidov, H. Kaji, H. Shiku, M. Ramalingam, K. Nakajima, Y. Sakka, A. Khademhosseini and T. Matsue, *Advanced Materials*, 2013, **25**, 4028-4034.
- F. Du, J. E. Fischer and K. I. Winey, *Departmental Papers (MSE)*, 2005, 79.
- T. Kimura, H. Ago, M. Tobita, S. Ohshima, M. Kyotani and M. Yumura, *Advanced materials*, 2002, **14**, 1380-1383.
- E. Sancaktar and N. Dilsiz, *Journal of adhesion science and technology*, 1997, **11**, 155-166.
- B. W. Steinert and D. R. Dean, *Polymer*, 2009, **50**, 898-904.
- D. Wang, P. Song, C. Liu, W. Wu and S. Fan, *Nanotechnology*, 2008, **19**, 075609.
- B. Z. Tang and H. Xu, *Macromolecules*, 1999, **32**, 2569-2576.
- C. Mao, J. Huang, Y. Zhu, W. Jiang, Q. Tang and X. Ma, *The Journal of Physical Chemistry Letters*, 2012, **4**, 43-47.
- J. Huang, Y. Zhu, W. Jiang, J. Yin, Q. Tang and X. Yang, *ACS applied materials & interfaces*, 2014.
- M. Gopinadhan, P. W. Majewski and C. O. Osuji, *Macromolecules*, 2010, **43**, 3286-3293.
- P. W. Majewski, M. Gopinadhan, W.-S. Jang, J. L. Lutkenhaus and C. O. Osuji, *Journal of the American Chemical Society*, 2010, **132**, 17516-17522.
- A. Anwer and A. H. Windle, *Polymer*, 1991, **32**, 103-108.
- S. A. Kossikhina, T. Kimura, E. Ito and M. Kawahara, *Polymer Engineering & Science*, 1998, **38**, 914-921.
- M. Gopinadhan, P. W. Majewski, E. S. Beach and C. O. Osuji, *ACS Macro Letters*, 2011, **1**, 184-189.
- C. Osuji, P. J. Ferreira, G. Mao, C. K. Ober, J. B. Vander Sande and E. L. Thomas, *Macromolecules*, 2004, **37**, 9903-9908.
- T. Pullawan, A. N. Wilkinson and S. J. Eichhorn, *Biomacromolecules*, 2012, **13**, 2528-2536.
- E. Choi, J. Brooks, D. Eaton, M. Al-Haik, M. Hussaini, H. Garmestani, D. Li and K. Dahmen, *Journal of Applied Physics*, 2003, **94**, 6034-6039.
- S. Jin, T. Tiefel and R. Wolfe, *Magnetics, IEEE Transactions on*, 1992, **28**, 2211-2213.
- S. Jin, R. Sherwood, J. Mottine, T. Tiefel, R. Opila and J. Fulton, *Journal of Applied Physics*, 1988, **64**, 6008-6010.
- H. Garmestani, M. S. Al - Haik, K. Dahmen, R. Tannenbaum, D. Li, S. S. Sablin and M. Y. Hussaini, *Advanced Materials*, 2003, **15**, 1918-1921.
- J. Sugiyama, H. Chanzy and G. Maret, *Macromolecules*, 1992, **25**, 4232-4234.
- D. Fragouli, A. Das, C. Innocenti, Y. Guttikonda, S. Rahman, L. Liu, V. Caramia, C. M. Megaridis and A.

## ARTICLE

Journal Name

- Athanassiou, *ACS applied materials & interfaces*, 2014, **6**, 4535-4541.
37. M. A. Guziak, Y. Honma, K. Hashimoto, T. Nishizaki, K. Watanabe and T. Sasaki, 2014.
38. S. Kaida, J. Matsui, T. Sagae, Y. Hoshikawa, T. Kyotani and T. Miyashita, *Carbon*, 2013, **59**, 503-511.
39. G. Chen, D. N. Futaba, S. Sakurai, M. Yumura and K. Hata, *Carbon*, 2014, **67**, 318-325.
40. K. van de Ruit, R. I. Cohen, D. Bollen, T. van Mol, R. Yerushalmi - Rozen, R. A. Janssen and M. Kemerink, *Advanced Functional Materials*, 2013, **23**, 5778-5786.
41. R. Tkacz, R. Oldenbourg, A. J. Fulcher, M. Miansari and M. Majumder, *The Journal of Physical Chemistry C*, 2013.
42. H. Zhang, L. Qiu, H. Li, Z. Zhang, Z. Yang and H. Peng, *Journal of colloid and interface science*, 2013, **395**, 322-325.
43. M. Cakmak, S. Batra and B. Yalcin, *Polymer Engineering & Science*, 2014.
44. G. Singh, S. Batra, R. Zhang, H. Yuan, K. G. Yager, M. Cakmak, B. Berry and A. Karim, *ACS nano*, 2013, **7**, 5291-5299.
45. S. Batra, University of Akron, 2014.
46. E. Unsal, J. Drum, O. Yucel, I. Nugay, B. Yalcin and M. Cakmak, *Review of Scientific Instruments*, 2012, **83**, 025114.